Progress In Electromagnetics Research, PIER 55, 285–306, 2005

INPUT ADMITTANCES ARISING FROM EXPLICIT SOLUTIONS TO INTEGRAL EQUATIONS FOR INFINITE-LENGTH DIPOLE ANTENNAS

G. Fikioris and C. A. Valagiannopoulos

Department of Electrical and Computer Engineering
National Technical University
GR 157-73 Zografou, Athens, Greece

Abstract—When one uses integral equations to determine the input admittance of dipole antennas, one must choose between two kernels, the exact and the approximate kernel, and also between (at least) two types of feed, the delta-function generator and the frill generator. For dipole antennas of infinite length, we investigate—analytically and numerically—the similarities and differences between the various admittance values. Particular emphasis is placed on the fact, discussed in detail in recent publications, that certain combinations lead to non-solvable integral equations.

1. INTRODUCTION

When applying moment methods to the Hallén-type equation for a cylindrical dipole of finite length and radius a, one must choose between the exact and the approximate (also called reduced) kernel. One must also choose between the delta-function generator [1] and more complex feeding structures, the most well-known of which is the frill generator of inner (outer) radius a (b) [2]. Thus, there are four possible integral equations. On these choices, see also the standard textbooks [3] and [4]. One must also choose a particular version of the method of moments (i.e. choose the basis and testing functions), as well as the number of basis/testing functions to be used. Generally speaking, the various choices lead to different values of input admittance.

As discussed in detail in refs. [1] and [2] (see also [5–7]) two of the above four integral equations, those involving the approximate kernel, lead to *non-solvable* integral equations. While use of the approximate kernel is widespread, the rather peculiar issue of insolvability accentuates the problem of choosing the basis/testing functions, as well as their number. When their number is very large, for example, erroneous oscillations occur near the driving point and/or near the ends of the antenna [1, 2]. (Such oscillations do not occur in the case of the exact kernel; certain considerations that help one choose the number of basis functions in that case are contained in [8].)

A basic tool employed in the aforementioned references [1] and [2] is the antenna of infinite length. There are still four choices of Hallén-type equations, only one (not two) of which is non-solvable. The three *solvable* integral equations can be solved explicitly using a Fourier transform, and the solutions take the form of convergent integrals. Furthermore, each convergent integral is also the solution to the corresponding integral equation of the Pocklington type. When applied to the *non-solvable* integral equation, on the other hand, the Fourier-transform method leads to a *divergent* integral. With the infinite antenna, therefore, one can simply use explicit solutions and need not worry about choosing the particular basis and testing functions, nor their number; furthermore, there is no difference between an integral equation of the Hallén type and its corresponding Pocklington-type counterpart.

In the present paper, we investigate the similarities and difference between admittance values obtained from the three solvable integral equations. As one might expect, separate investigations for input conductance and susceptance are required. Perhaps unexpectedly, it is possible to define an input conductance (but not a susceptance) for the non-solvable case; this conductance is also investigated in the present paper.

Studies of infinite-length structures are common in electromagnetics, and infinite-antenna models have been extensively studied by many authors. See, for example, [9–22]; additional references, as well as several reasons motivating such studies are given in [20]. The motivation, purpose and methods of the present paper are different from the above-mentioned references: The specific starting points of the present study are the infinite-antenna results of [1] and [2].

Our time dependence is $e^{-i2\pi ft}$, where $k = 2\pi/\lambda = 2\pi f/c$.

2. FOURIER TRANSFORMS OF THE KERNELS

Fourier transforms—in which the spatial variable z is transformed to the Fourier variable ζ—are used extensively in this paper. For real ζ, the Fourier transforms of the approximate and exact kernels are [2]

$$\bar{K}_{\rm ap}(\zeta, a) = \begin{cases} \dfrac{i}{4} H_0^{(1)}(a\sqrt{k^2 - \zeta^2}), & \text{if } |\zeta| < k \\ \dfrac{1}{2\pi} K_0(a\sqrt{\zeta^2 - k^2}), & \text{if } |\zeta| > k, \end{cases} \tag{1}$$

and

$$\bar{K}_{\rm ex}(\zeta,a)=\begin{cases}\dfrac{i}{4}J_0(a\sqrt{k^2-\zeta^2})H_0^{(1)}(a\sqrt{k^2-\zeta^2}), & \text{if } |\zeta|<k\\ \dfrac{1}{2\pi}I_0(a\sqrt{\zeta^2-k^2})K_0(a\sqrt{\zeta^2-k^2}), & \text{if } |\zeta|>k.\end{cases} \tag{2}$$

For brevity, these Fourier transforms will be referred to simply as "kernels." For each kernel, the top ($|\zeta|<k$) and bottom ($|\zeta|>k$) formulas are analytic continuations of one another. Both kernels are real when ζ is real and $|\zeta|>k$. Finally, the branch cut originating from $\zeta=k$ ($\zeta=-k$) lies in the upper-half (lower-half) ζ-plane [5].

For large, positive ζ, the asymptotic behavior of the kernels is found from the large-argument formulas for K_0 and I_0K_0 [23, 9.7.2, 9.7.5] to be

$$\bar{K}_{\rm ap}(\zeta,a)\sim\frac{1}{\sqrt{8\pi a}}\frac{e^{-a\zeta}}{\sqrt{\zeta}},\quad \text{as } \zeta\to+\infty, \tag{3}$$

and

$$\bar{K}_{\rm ex}(\zeta,a)\sim\frac{1}{4\pi a}\frac{1}{\zeta},\quad \text{as } \zeta\to+\infty. \tag{4}$$

We will also be interested in the asymptotic behavior of the kernels as $\zeta\to k$. Throughout this paper, when discussing this limit we assume that ζ remains in the lower-half plane so that ζ approaches k from below. From the small-argument formula for $H_0^{(1)}$ [23, 9.1.3, 9.1.12, 9.1.13] or, alternatively, from the corresponding formula for K_0 [23, 9.6.12, 9.6.13], it is seen that

$$\bar{K}_{\rm ap}(\zeta,a)=-\frac{1}{4\pi}\ln(\zeta-k)+O(1),\quad \text{as } \zeta\to k. \tag{5}$$

For the same reasons, an identical relation holds for the exact kernel

$$\bar{K}_{\rm ex}(\zeta,a)=-\frac{1}{4\pi}\ln(\zeta-k)+O(1),\quad \text{as } \zeta\to k. \tag{6}$$

3. EXPLICIT FORMULAS FOR THE CURRENTS

The purpose of this section is to give the explicit formulas for the currents. These formulas are integrals, and their convergence properties are discussed.

3.1. Delta-Function Generator

Consider the case of the delta-function generator first. With the exact kernel, the current $I^{(\infty)}_{\mathrm{ex},\delta}(z)$ satisfies an integral equation of the Hallén type, as well as one of the Pocklington type. The explicit solution to either equation is [1]

$$I^{(\infty)}_{\mathrm{ex},\delta}(z) = \frac{ikV}{\pi\zeta_0}\int_{0,(k)}^{\infty} \frac{\cos\zeta z}{(k^2-\zeta^2)\bar{K}_{\mathrm{ex}}(\zeta,a)}\,d\zeta, \tag{7}$$

where $\zeta_0 = 376.73\,\Omega$hms, and where the notation $\int_{0,(k)}^{\infty}$ means that the integration path passes below the singularity at $\zeta = k$ in the complex ζ-plane, while starting at 0 and ending at $+\infty$ (note that there is a typographical error in the relevant [1, eqn. (15)]). Bypassing $\zeta = k$ is necessary because of (6), which shows that the integrand has a non-integrable singularity at $\zeta = k$. By (4), eqn. (7) defines an integral which converges (conditionally) for all real z except $z = 0$—more on this later. In Appendix A a useful, alternative representation for $I^{(\infty)}_{\mathrm{ex},\delta}(z)$—as a Cauchy Principal Value integral—is obtained.

The situation is completely different for the approximate kernel [1, 5]: If one replaces $\bar{K}_{\mathrm{ex}}(\zeta,a)$ by $\bar{K}_{\mathrm{ap}}(\zeta,a)$ in (7), one obtains an integral which, because of (3), diverges for all real z. Thus, with the approximate kernel (still with the delta-function generator), the integral equation is non-solvable, and there is no well-defined current.

3.2. Frill Generator

Similarly, with the exact kernel/frill generator combination, one has an explicit solution $I^{(\infty)}_{\mathrm{ex,fr}}(z)$. Although "most" integral equations that use the approximate kernel are non-solvable [2], the combination infinite antenna/approximate kernel/*frill generator* surprisingly yields a solvable integral equation. If the solution is $I^{(\infty)}_{\mathrm{ap,fr}}(z)$, then, in concise notation, the two solutions can be written together as [2]

$$I^{(\infty)}_{\mathrm{ex/ap,fr}}(z) = \frac{2ikV}{\zeta_0\ln(b/a)}\int_{0,(k)}^{\infty} \frac{\left[\bar{K}_{\mathrm{ap}}(\zeta,a)-\bar{K}_{\mathrm{ap}}(\zeta,b)\right]\cos\zeta z}{(k^2-\zeta^2)\bar{K}_{\mathrm{ex/ap}}(\zeta,a)}\,d\zeta, \tag{8}$$

where, in the denominator of the integrand, one uses $\bar{K}_{\mathrm{ex}}(\zeta,a)$ to find $I^{(\infty)}_{\mathrm{ex,fr}}(z)$ and $\bar{K}_{\mathrm{ap}}(\zeta,a)$ to find $I^{(\infty)}_{\mathrm{ap,fr}}(z)$. Note that the terms in the *numerator* of the integrand always involve the *approximate* kernel; these terms originate from the right-hand side of the integral equation. Once again, there is a non-integrable singularity at $\zeta = k$ which is

bypassed in the usual manner. We note that a principal-value integral representation—similar to (A3) of Appendix A—is possible once again. Finally, it is worth pointing out something not mentioned in [2]: With the approximate kernel, the right-hand side of eqn. (8) appears, in a different context, in [13, eqn. (26)].

4. EXPLICIT FORMULAS FOR INPUT ADMITTANCE

There are four combinations of kernel and feed. For all combinations leading to a well-defined input conductance or susceptance, we now give the relevant formula(s). When a particular combination does not lead to a well-defined input conductance or susceptance, we give the reason.

4.1. Exact Kernel/Delta-Function Generator

For the exact kernel/delta-function generator combination, as one approaches the driving point, the imaginary part of $I^{(\infty)}_{\mathrm{ex},\delta}(z)/V$ becomes infinite (logarithmically) because of the infinitesimal gap [1, 5], so that the input susceptance is undefined. The real part, however, remains finite and, at $z = 0$, gives the following input conductance $G^{(\infty)}_{\mathrm{ex},\delta}$

$$G^{(\infty)}_{\mathrm{ex},\delta} = \frac{4k}{\pi\zeta_0}\int_0^k \frac{d\zeta}{(k^2-\zeta^2)\left[J_0^2(a\sqrt{k^2-\zeta^2})+Y_0^2(a\sqrt{k^2-\zeta^2})\right]}. \qquad (9)$$

Eqn. (9) can be deduced from [5] or [24]. The latter reference also contains a brief derivation (note, however, some essential changes in notation). Appendix A provides an improved, more elegant derivation, which proceeds from the aforementioned principal-value integral representation of $I^{(\infty)}_{\mathrm{ex},\delta}(z)$. That derivation will form the basis for other results in this paper.

4.2. Exact Kernel/Frill Generator

With this combination, the input admittance $G^{(\infty)}_{\mathrm{ex,fr}} + iB^{(\infty)}_{\mathrm{ex,fr}}$ can be found immediately from (8). It is given by the convergent integral

$$G^{(\infty)}_{\mathrm{ex,fr}} + iB^{(\infty)}_{\mathrm{ex,fr}} = \frac{2ik}{\zeta_0\ln(b/a)}\int_{0,(k)}^{\infty} \frac{\bar{K}_{\mathrm{ap}}(\zeta,a)-\bar{K}_{\mathrm{ap}}(\zeta,b)}{(k^2-\zeta^2)\bar{K}_{\mathrm{ex}}(\zeta,a)}\,d\zeta. \qquad (10)$$

If one applies the procedure of Appendix A starting from (8) (instead of (7)), it is possible to come up with a formula for $G^{(\infty)}_{\mathrm{ex,fr}}$ as an integral from 0 to k (similar, that is, to (9)), but we will not dwell on this point.

4.3. Approximate Kernel/Delta-Function Generator

With the approximate kernel/delta-function generator combination, the integral equation is non-solvable. One can, however, define an input *conductance* $G^{(\infty)}_{\mathrm{ap},\delta}$ by the following sequence of steps [1]. (i) Apply Galerkin's method with pulse functions to the integral equation; let z_0 be the pulse width. (ii) Divide the "Galerkin solution" (for the current) thus obtained by the driving voltage V. (iii) Take the limit of the *real* part as $z_0 \to 0$ (the limit of the imaginary part is, of course, infinite). (iv) Finally, set $z = 0$. One finally obtains [1] (also, [24]; but note the notation differences)

$$G^{(\infty)}_{\mathrm{ap},\delta} = \frac{4k}{\pi\zeta_0}\int_0^k \frac{J_0(a\sqrt{k^2-\zeta^2})}{(k^2-\zeta^2)\left[J_0^2(a\sqrt{k^2-\zeta^2})+Y_0^2(a\sqrt{k^2-\zeta^2})\right]}\,d\zeta, \tag{11}$$

which differs from (9) only in the J_0 in the numerator of the integrand.

The above sequence of steps immediately gives rise to the question: Would a numerical method other than Galerkin's method with pulse functions give a different input conductance? The answer seems to be no: The discussion in [5, Section 8.5] shows that $G^{(\infty)}_{\mathrm{ap},\delta}$ is actually a method-independent quantity.

4.4. Approximate Kernel/Frill Generator

With the approximate kernel/frill generator combination, the input admittance is obtained from (8) as

$$G^{(\infty)}_{\mathrm{ap,fr}} + iB^{(\infty)}_{\mathrm{ap,fr}} = \frac{2ik}{\zeta_0\ln(b/a)}\int_{0,(k)}^{\infty}\frac{\bar{K}_{\mathrm{ap}}(\zeta,a)-\bar{K}_{\mathrm{ap}}(\zeta,b)}{(k^2-\zeta^2)\bar{K}_{\mathrm{ap}}(\zeta,a)}\,d\zeta. \tag{12}$$

The only difference from the exact-kernel case (10) is that $\bar{K}_{\mathrm{ap}}(\zeta,a)$ appears in place of $\bar{K}_{\mathrm{ex}}(\zeta,a)$ in the denominator of the integrand. Once again, it is possible to find a formula for $G^{(\infty)}_{\mathrm{ap,fr}}$ as an integral from 0 to k.

5. LIMITING CASES

5.1. The Small-Frill Limit: General Formulas

For any antenna radius a, the delta-function generator is infinitesimally small in size (height). One might thus be led to believe that the current (admittance) due to an infinitesimally small frill generator—limit $b \to a$, to be referred to as "small-frill limit" and indicated by

the subscript 'smfr'—would reduce to the current (admittance) due to the delta-function generator. We will show here that this is not the case: Assuming that the kernel remains the same, the limiting values of current and admittance are different. We will then take a further step and come up with an unexpected relation between the small-frill limit and the delta-function generator case.

In (8), replace $\ln(b/a)$ and $\bar{K}_{\rm ap}(\zeta,a)-\bar{K}_{\rm ap}(\zeta,b)$ by the first nonzero term in their respective Taylor-series expansion about the point $b=a$ to obtain

$$I^{(\infty)}_{\rm ex/ap,smfr}(z) = -\frac{2ikaV}{\zeta_0}\int_{0,(k)}^{\infty}\frac{g(\zeta,a)\cos\zeta z}{(k^2-\zeta^2)\bar{K}_{\rm ex/ap}(\zeta,a)}\,d\zeta, \tag{13}$$

where $g(\zeta,a)=\partial\bar{K}_{\rm ap}(\zeta,a)/\partial a$. This derivative can be obtained with (1) and the formulas [23, eqns. 9.1.28 and 9.6.27] for the derivatives of $H_0^{(1)}$ and K_0. It is

$$g(\zeta,a)=\begin{cases} -\dfrac{i}{4}\left(k^2-\zeta^2\right)^{1/2}H_1^{(1)}(a\sqrt{k^2-\zeta^2}), & \text{if } |\zeta|<k \\ -\dfrac{1}{2\pi}\left(\zeta^2-k^2\right)^{1/2}K_1(a\sqrt{\zeta^2-k^2}), & \text{if } |\zeta|>k. \end{cases} \tag{14}$$

In (14), the top ($|\zeta|<k$) and bottom ($|\zeta|>k$) formulas are, once again, analytic continuations of one another. Furthermore, g is real when ζ is real and $|\zeta|>k$.

The asymptotic behavior of $g(\zeta,a)$ near $\zeta=k$ can be found from the small-argument formula for $H_1^{(1)}$ [23, 9.1.3, 9.1.10, 9.1.11], or, alternatively, from the corresponding formula for K_1 [23, 9.6.10, 9.6.11]. It is

$$g(\zeta,a) = -\frac{1}{2\pi a}+O\left[(\zeta-k)\ln(\zeta-k)\right], \quad \text{as } \zeta\to k. \tag{15}$$

The point $\zeta=k$ is, once again, a non-integrable singularity and is bypassed in (13).

For large, positive ζ, the asymptotic behavior of $g(\zeta,a)$ can be found from the large-argument formula [23, 9.7.2] for K_1 to be

$$g(\zeta,a)\sim -\frac{1}{\sqrt{8\pi a}}e^{-a\zeta}\sqrt{\zeta}, \quad \text{as } \zeta\to+\infty. \tag{16}$$

So far, the results in this section hold for both kernels. We now specialize.

5.2. The Small-Frill Limit: Exact Kernel

For the case of the exact kernel, from (16) and (4) it is seen that the integrand in (13) decays exponentially, so that the integral converges for all real z. Because the current $I^{(\infty)}_{\mathrm{ex,smfr}}(z)$ in (13) is different from the current $I^{(\infty)}_{\mathrm{ex},\delta}(z)$ in (7), the current due to the small frill is, indeed, different from the current due to the delta-function generator. The input admittance corresponding to the present case is

$$G^{(\infty)}_{\mathrm{ex,smfr}} + iB^{(\infty)}_{\mathrm{ex,smfr}} = -\frac{2ika}{\zeta_0}\int_{0,(k)}^{\infty} \frac{g(\zeta,a)}{(k^2-\zeta^2)\bar{K}_{\mathrm{ex}}(\zeta,a)}\,d\zeta. \tag{17}$$

One can go further and find formulas for the conductance. This is done in Appendix B—the procedure resembles that of Appendix A. The final result is

$$G^{(\infty)}_{\mathrm{ex,smfr}} = \frac{4k}{\pi\zeta_0}\int_0^k \frac{d\zeta}{(k^2-\zeta^2)\,J_0(a\sqrt{k^2-\zeta^2})\left[J_0^2(a\sqrt{k^2-\zeta^2})+Y_0^2(a\sqrt{k^2-\zeta^2})\right]}, \tag{18}$$

which differs from (9) only by the extra J_0 in the denominator. From (9) and the small argument formula [23, 9.1.12] of J_0, it is apparent that

$$G^{(\infty)}_{\mathrm{ex,smfr}} - G^{(\infty)}_{\mathrm{ex},\delta} = O(a^2), \quad \text{as } a \to 0, \tag{19}$$

so that the two conductances are very close to one another, and the difference vanishes for small antenna radius.

5.3. The Small-Frill Limit: Approximate Kernel

Eqns. (16) and (3) show that, with the approximate kernel, the integrand in (13) is of order $\cos\zeta z/\zeta$ for large, positive ζ. Thus, the integral converges for all real z except $z = 0$, and gives the current due to the small frill. With the same kernel, the corresponding current due to the delta-function generator is not well-defined. Thus, with the approximate kernel, the small frill is clearly different from the delta-function generator.

The conductance for this case is determined in Appendix C—the approach is very similar to that of Appendix B. One is lead precisely to the expression on the RHS of (9), so that

$$G^{(\infty)}_{\mathrm{ap,smfr}} = G^{(\infty)}_{\mathrm{ex},\delta}. \tag{20}$$

We have thus reached the surprising (at least to us!) conclusion that *both*
(i) replacing the small frill by a delta-function generator *and*
(ii) replacing the approximate kernel by the exact kernel,
leaves the input conductance (or, more generally, the real part of $I^{(\infty)}(z)/V$) unaltered (but any *single one* of the above two replacements changes the conductance.) There seems to be no simple physical explanation of the equality (20). Finding such an explanation is hindered by the fact that there is no similar equality for the *imaginary* part of $I^{(\infty)}(z)/V$ (at $z = 0$, the susceptance $\mathrm{Im}\{I^{(\infty)}(0)/V\}$ remains, in both cases, undefined).

5.4. The Thin-Antenna, Small-Frill Limit

We now consider the case where both the antenna is thin and the frill is small. Specifically, consider that $a \to 0$ and $b \to 0$ while $b/a =$fixed, a situation to be described as the "thin-antenna, small-frill limit." Let $\mu = b/a$. It is a consequence of the small-argument formula for $H_0^{(1)}$ or, alternatively, of the corresponding formula for K_0 that

$$\bar{K}_{\mathrm{ap}}(\zeta, a) - \bar{K}_{\mathrm{ap}}(\zeta, \mu a) \sim \frac{1}{2\pi} \ln \mu, \quad \text{as } a \to 0 \text{ with } \mu \text{ fixed.} \tag{21}$$

As a consequence of (8) and (21), in the limit $b \to a$ with $b/a =$fixed, one has

$$I^{(\infty)}_{\mathrm{ex/ap,fr}}(z) \sim \frac{ikV}{\pi\zeta_0} \int_{0,(k)}^{\infty} \frac{\cos \zeta z}{(k^2 - \zeta^2)\bar{K}_{\mathrm{ex/ap}}(\zeta, a)}\, d\zeta. \tag{22}$$

With the exact kernel, the integral on the RHS of (22) is precisely the current (7) for the case of the delta-function generator. With the approximate kernel, the integral on the RHS of (22) diverges. Thus, for both kernels, the thin-antenna, small-frill limit reduces to the thin-antenna limit of the delta-function generator. This is a natural result.

6. NUMERICAL CALCULATION OF INTEGRALS

The numerical results of this paper (next Section 7) are for input admittance. The results were obtained by calculating the integrals of the previous Sections 4 and 5 numerically. In this section, we describe our numerical integration schemes.

6.1. Integrals for Conductance

Consider, first the integrals in (9), (11), and (18), which represent, respectively, the input conductances $G^{(\infty)}_{\mathrm{ex},\delta}$, $G^{(\infty)}_{\mathrm{ap},\delta}$, and $G^{(\infty)}_{\mathrm{ex,smfr}}$. We used several schemes for these integrals, and compared the results. One successful scheme results by a change of variable $\zeta/k = \sqrt{1-t^2}$ so that (9), for example, is converted to

$$G^{(\infty)}_{\mathrm{ex},\delta} = \frac{4}{\pi\zeta_0}\int_0^1 \frac{dt}{t\sqrt{1-t^2}\left[J_0^2(kat)+Y_0^2(kat)\right]}. \tag{23}$$

The integration path is a finite portion of the real axis, on which the integrand is real and analytic. Singularities occur only at the endpoints: The integrand behaves like $1/\sqrt{1-t}$ near $t=1$ and like $1/[t(\ln t)^2]$ near $t=0$. Both singularities are, of course, integrable (integrability in the latter case is discussed in Appendix A), and can be handled by appropriate, adaptive numerical integration routines.

6.2. Integrals for Admittance

Less straightforward are the complex integrals in (10), (12), and (17), which represent input admittance (both conductance and susceptance). By (3), (4), and (16), the integrands in (10) and (17) decrease exponentially for large, positive ζ. This desirable property does not hold for the integrand in (12), but the difficulty is easily circumvented if one splits the integral into two and evaluates the first in closed form. The result is

$$G^{(\infty)}_{\mathrm{ap,fr}} + iB^{(\infty)}_{\mathrm{ap,fr}} = \frac{\pi}{\zeta_0\ln(b/a)}\left[1 - \frac{2ik}{\pi}\int_{0,(k)}^{\infty}\frac{\bar{K}_{\mathrm{ap}}(\zeta,b)}{(k^2-\zeta^2)\bar{K}_{\mathrm{ap}}(\zeta,a)}\,d\zeta\right], \tag{24}$$

in which the new integrand is exponentially decreasing.

The integrals (10), (17), and (24) were calculated by bypassing the non-integrable singularity at $\zeta = k$ by a well-shaped path lying in the lower-half plane. The integral is, of course, independent of the well's height and length, and these parameters were varied as a check. Lastly, we integrated up to a finite upper limit $\zeta_{\max}$ which we increased until "convergence;" because of the integrands' exponential decrease, the finally required value of $\zeta_{\max}$ was not particularly large.

7. ADMITTANCE: SELECTED NUMERICAL RESULTS

In this section, we present numerical results as function of the two parameters a/λ and b/λ. The values of a/λ is always taken to

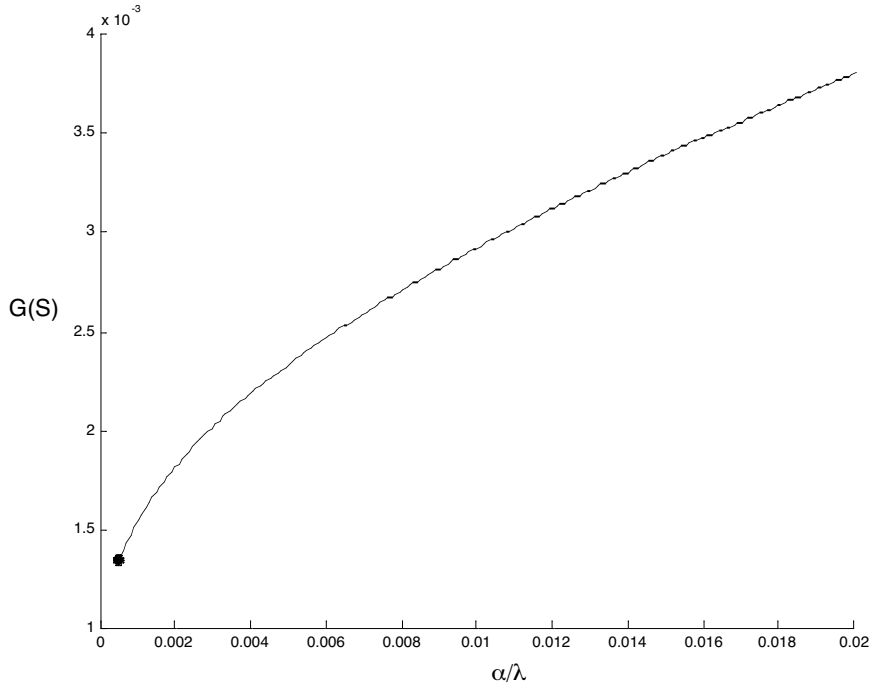

Figure 1. Input conductances $G^{(\infty)}_{\mathrm{ex},\delta}$ and $G^{(\infty)}_{\mathrm{ap,smfr}}$ (by eqn. (20), the two quantities are equal) as function of the electrical radius a/λ. The leftmost point corresponds to $a/\lambda = 0.0005$; smaller values of a/λ lead to smaller values of conductance.

be smaller than 0.02 (note, however, that the *approximate* kernel is ordinarily used up to $a/\lambda = 0.01$ only [1, 25]). The value of b/λ is such that the single-mode (TEM) assumption of the coaxial line always holds (i.e., the TE_{11} mode, which is the next mode, cannot propagate).

7.1. b-Independent Quantities

Fig. 1 shows the input conductance $G^{(\infty)}_{\mathrm{ex},\delta}$ (similar results for this quantity can also be found in [14]) which, by eqn. (20), is equal to $G^{(\infty)}_{\mathrm{ap,smfr}}$. The percentage differences between this quantity and the other two b-independent conductances $G^{(\infty)}_{\mathrm{ap},\delta}$ and $G^{(\infty)}_{\mathrm{ex,smfr}}$ are shown in Fig. 2. In accordance with eqn. (19), the differences increase with increasing a/λ. Perhaps unexpectedly, all quantities are seen to be extremely close to one another: The largest difference (it occurs

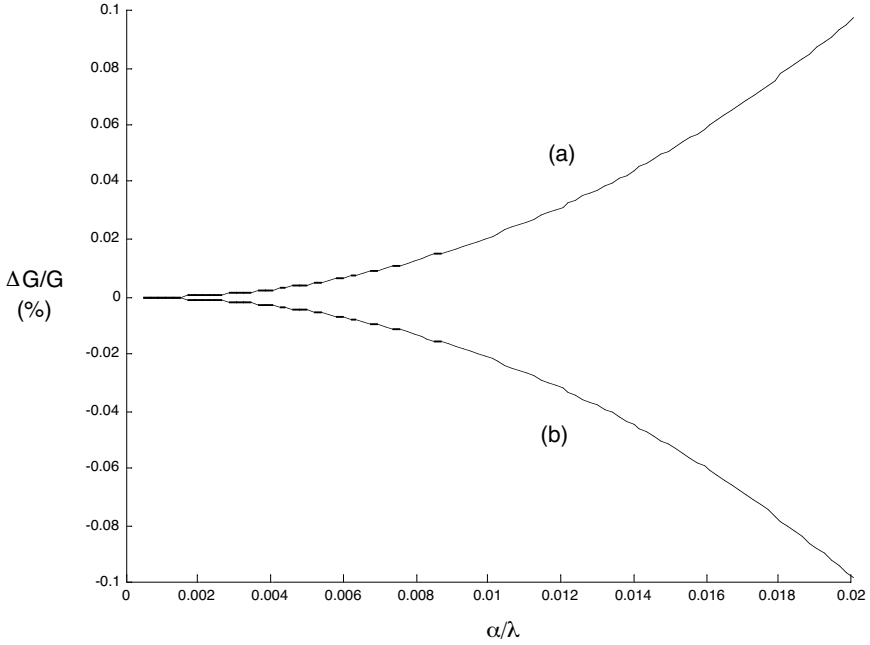

Figure 2. Percentage errors (a) between conductances $G^{(\infty)}_{\mathrm{ex},\delta}$ and $G^{(\infty)}_{\mathrm{ap},\delta}$ (top curve) and (b) between conductances $G^{(\infty)}_{\mathrm{ex},\delta}$ and $G^{(\infty)}_{\mathrm{ex,smfr}}$ (bottom curve).

between the quantities $G^{(\infty)}_{\mathrm{ap},\delta}$ and $G^{(\infty)}_{\mathrm{ex,smfr}}$) is only 0.2% for the thickest antenna ($a/\lambda = 0.02$). These results show that the input conductances in the small-frill limit are *numerically* very close to those of the delta-function generator.

The only input susceptance which is independent of b is $B^{(\infty)}_{\mathrm{ex,smfr}}$; it will be plotted together with other quantities in Fig. 6 below.

7.2. Quantities that Depend on b

The above-discussed quantities do not depend on b and the picture that emerges is very simple. By contrast, the overall picture that emerges from the quantities that do depend on b is quite complicated. Out of the many numerical results we have obtained, the ones to be shown have been selected to illustrate and supplement what we have found analytically.

Fig. 3 shows the b-dependent conductances $G^{(\infty)}_{\mathrm{ex,fr}}$ and $G^{(\infty)}_{\mathrm{ap,fr}}$

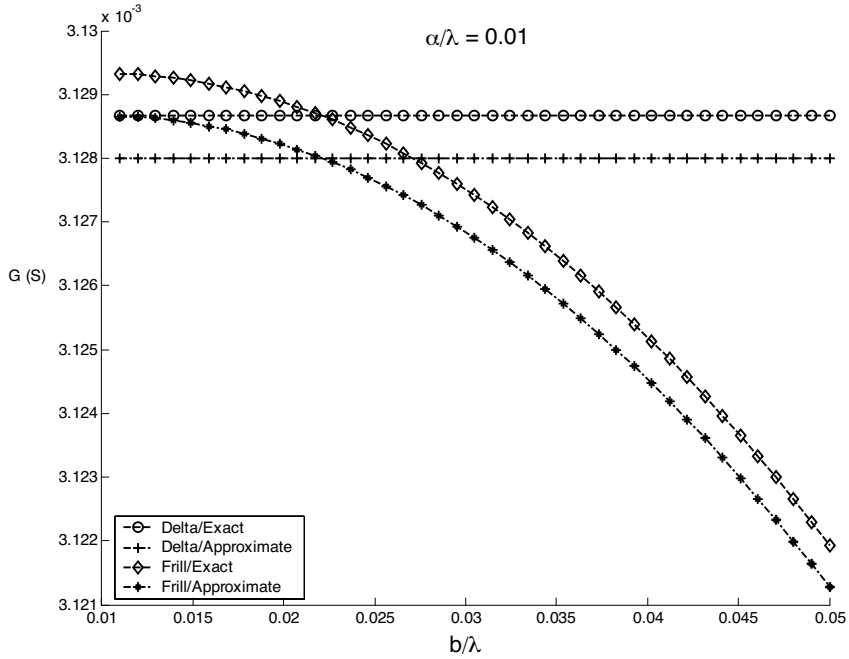

Figure 3. b-dependent conductances $G^{(\infty)}_{\mathrm{ex,fr}}$ and $G^{(\infty)}_{\mathrm{ap,fr}}$ together with the b-independent $G^{(\infty)}_{\mathrm{ex},\delta}$ and $G^{(\infty)}_{\mathrm{ap},\delta}$ as function of b/λ, for fixed $a/\lambda = 0.01$.

together with the b-independent $G^{(\infty)}_{\mathrm{ex},\delta}$ and $G^{(\infty)}_{\mathrm{ap},\delta}$ for fixed $a/\lambda = 0.01$. The varying parameter is b/λ. The leftmost part of this curve corresponds to the small-frill limit; thus, the analysis of Sections 5.2 and 5.3 explains the coincidence, at left, of $G^{(\infty)}_{\mathrm{ex},\delta}$ and $G^{(\infty)}_{\mathrm{ap,fr}}$. It also explains the non-coincidence, at left, of the other quantities. As one moves toward the right (i.e., for larger values of b/λ), there are some crossovers and after these, the differences grow. *Once again, the overall differences remain very, very small.*

Fig. 4 shows the four conductances, this time for varying a/λ and fixed $b/a = 10$. The results separate into two groups, one involving the frill, and one involving the delta-function generator. This rather large value $b/a = 10$ was so chosen so that the differences can be distinguished graphically (smaller values of b/a lead to smaller differences between the two groups). The analysis of Section 5.4 explains the coincidence at left.

It is very well known that input susceptance is generally a more

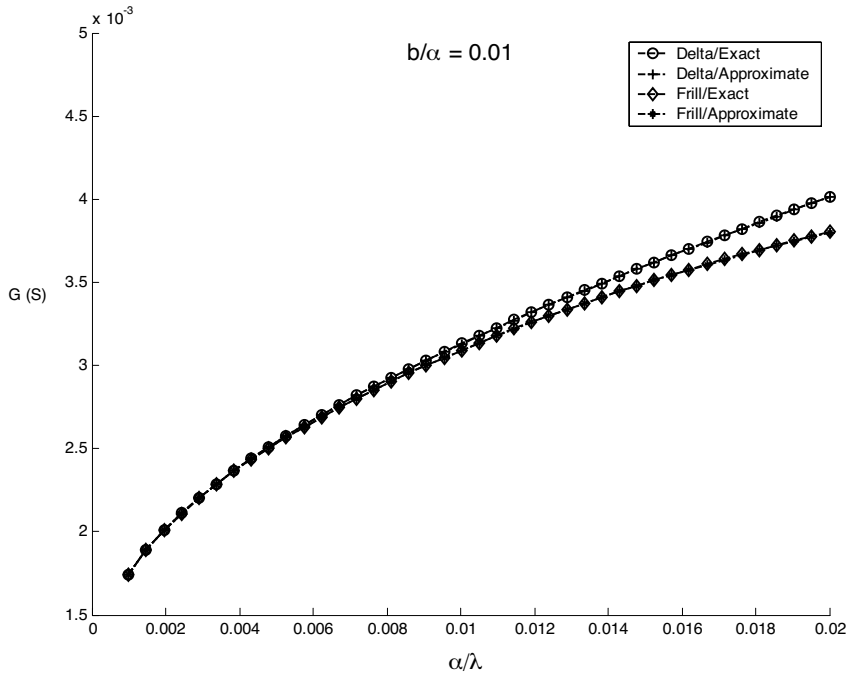

Figure 4. The four conductances of Fig. 5 for varying a/λ. For $G^{(\infty)}_{\mathrm{ex,fr}}$ and $G^{(\infty)}_{\mathrm{ap,fr}}$, b/a is fixed and equal to 10.

sensitive quantity than input conductance, and the infinite antennas considered here present no exception to this. For $b > a$, there are two well-defined input susceptances, $B^{(\infty)}_{\mathrm{ex,fr}}$ and $B^{(\infty)}_{\mathrm{ap,fr}}$. They are shown in Fig. 5 as function of a/λ, for fixed $b/a = 2$. As expected, the difference vanishes at left. *As opposed to the conductances, the differences here are quite large:* When $a/\lambda = 0.01$ (middle of diagram), the difference is 14%. As one might expect, the difference decreases as b/a increases: When $b/a = 5$, it is 7% and when $b/a = 1.01$, it is 45%.

In Fig. 6, the two b-dependent susceptances are shown, once again, for varying a/λ. This time, b/λ is fixed and equal to 0.011. Also shown is the b-independent quantity $B^{(\infty)}_{\mathrm{ex,smfr}}$ which, naturally, coincides at right with $B^{(\infty)}_{\mathrm{ex,fr}}$. The discussion in Section 5.C and the fact that the rightmost part corresponds to the small-frill limit explain why $B^{(\infty)}_{\mathrm{ap,fr}}$ appears to diverge at right.

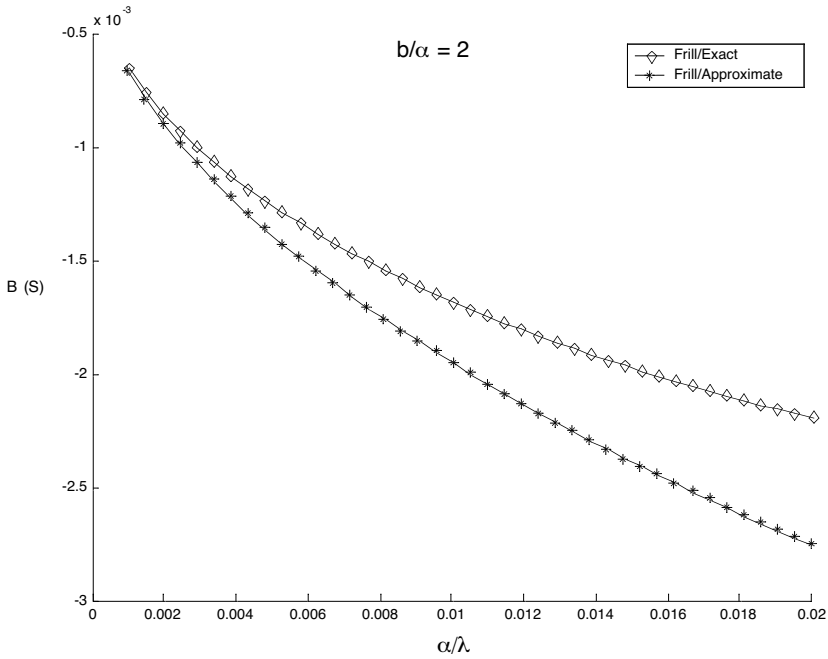

Figure 5. The two susceptances $B^{(\infty)}_{\text{ex,fr}}$ and $B^{(\infty)}_{\text{ap,fr}}$ as function of a/λ, for fixed $b/a = 2$.

8. CONCLUSION

In this paper, the driven dipole antenna of infinite length was considered. There are two choices of kernel in the integral equations for the current distribution, the exact and the approximate kernel, and two choices of feed, the delta-function generator and the frill generator. Out of the four possible integral equations, three are solvable whereas one (delta-function generator/approximate kernel) is not. Hallén and Pocklington-type integral equations are equivalent. All solvable integral equations can be solved explicitly.

It is possible to define an input conductance (G) for all three solvable cases. It is also possible to define a G for the non-solvable case; to do this, one applies a particular numerical method (Galerkin's method with pulse functions) to the integral equations and then takes the limit of the numerical solution as the pulse width goes to zero; in all likelihood, this definition is actually method-independent. Input susceptances (B) can be defined only for the two cases involving the frill generator.

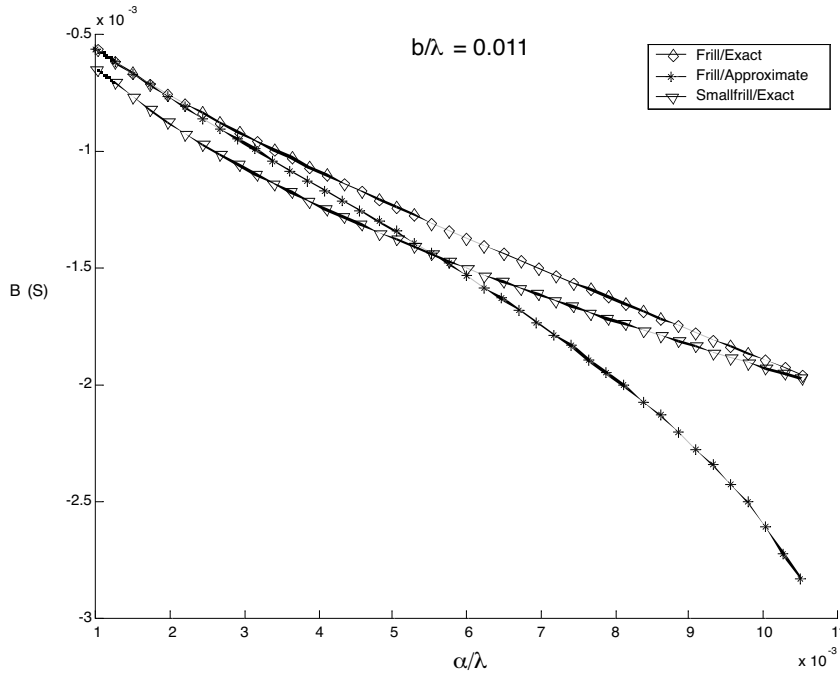

Figure 6. The two b-dependent susceptances $B^{(\infty)}_{\mathrm{ex,fr}}$ and $B^{(\infty)}_{\mathrm{ap,fr}}$ as function of a/λ, for fixed $b/\lambda = 0.011$. Also shown is the b-independent quantity $B^{(\infty)}_{\mathrm{ex,smfr}}$.

The aforementioned expressions for G and B take the form of convergent complex integrals involving the antenna radius a/λ and, in the case of the frill generator, the outer radius b/λ. When it is required to integrate to infinity, it is always possible to find forms with exponentially decreasing integrands. All integrals can be computed numerically, and interesting limiting cases can be studied analytically. Our numerical and analytical investigations show that the G's for the various cases are very close to one another, while certain B's can differ significantly. They also show that G for the delta-function generator/exact kernel combination *exactly* coincides with the limiting value, as $b \to a$, of G for the frill generator/approximate kernel case. On the other hand, the "small-frill limit" $b \to a$ does not *exactly* reduce to the delta-function generator case when the kernel remains the same. Such a reduction happens only when both a and b tend to zero, while b/a remains fixed, a situation referred to in this paper as the "thin-antenna, small-frill limit".

ACKNOWLEDGMENT

This work was supported, in part, by the EPEAEK Pythagoras Research Program. The work of CAV came from his Senior Thesis at the National Technical University.

APPENDIX A. ALTERNATIVE REPRESENTATION FOR $I_{\mathrm{ex},\delta}^{(\infty)}(Z)$; DERIVATION OF (9)

Here, we write (7) as a Cauchy Principal Value integral and use this to derive (9). Assume initially that $z \neq 0$. Denote the integrand of $I_{\mathrm{ex},\delta}^{(\infty)}(z)/V$ in (7) by $r(\zeta)$, so that

$$r(\zeta) = \frac{ik}{\pi\zeta_0} \frac{\cos\zeta z}{(k^2-\zeta^2)\bar{K}_{\mathrm{ex}}(\zeta,a)}. \tag{A1}$$

From (A1) and (6) it is seen that

$$r(\zeta) = \frac{2i\cos kz}{\zeta_0} \frac{1}{(\zeta-k)\ln(\zeta-k)} + O\left(\frac{1}{(\zeta-k)[\ln(\zeta-k)]^2}\right), \tag{A2}$$

as $\zeta \to k$ in the lower-half ζ-plane. Let L_ϵ be a path that starts at $k-\epsilon$ ($\epsilon > 0$), ends at $k+\epsilon$, and lies entirely in the lower-half ζ-plane. The leading term in (A2) is non-integrable. Nonetheless, one can readily show that, *due to the symmetric integration limits,* the limit as $\epsilon \to 0$ of the integral of this term along the path L_ϵ exists and equals zero. The remaining part in (A2) is integrable (to verify this, perform the integral $\int_A^k \frac{d\zeta}{(k-\zeta)[\ln(k-\zeta)]^2}$ by setting $k-\zeta = e^{-t}$; here, A is a real number close to k), so that the limit of its integral equals zero as well.

We have thus shown that $\lim_{\epsilon\to 0}\int_{L_\epsilon} r(\zeta)\,d\zeta = 0$; as a consequence,

$$\frac{I_{\mathrm{ex},\delta}^{(\infty)}(z)}{V} = \lim_{\epsilon\to 0}\left[\int_0^{k-\epsilon} r(\zeta)\,d\zeta + \int_{k+\epsilon}^{\infty} r(\zeta)\,d\zeta\right], \tag{A3}$$

so that $I_{\mathrm{ex},\delta}^{(\infty)}(z)/V$ has been written as a Cauchy Principal Value integral [26]. † The second integral in (A3) is purely imaginary. It necessarily follows that

$$\mathrm{Re}\left\{\frac{I_{\mathrm{ex},\delta}^{(\infty)}(z)}{V}\right\} = \int_0^k \mathrm{Re}\{r(\zeta)\}\,d\zeta, \tag{A4}$$

† Here, unlike many other applications [26–28], the integrand $r(\zeta)$ does not have a simple pole at $\zeta = k$, but behaves in accordance with (A2).

where no $\lim_{\epsilon\to 0}$ is required. The quantity $\mathrm{Re}\{r(\zeta)\}$ can be calculated with the aid of (A1) and (2), and with $G^{(\infty)}_{\mathrm{ex},\delta} = \mathrm{Re}\{I^{(\infty)}_{\mathrm{ex},\delta}(0)/V\}$, eqn. (9) has been derived. The restriction $z \neq 0$ can be removed in the real part of $I^{(\infty)}_{\mathrm{ex},\delta}(z)/V$ only.

APPENDIX B. DERIVATION OF (18)

The derivation of (18) closely parallels the derivation in Appendix A. From (13) with the exact kernel, the integrand $r(\zeta)$ of $I^{(\infty)}_{\mathrm{ex,smfr}}(z)/V$ is

$$r(\zeta) = \left(-\frac{2ika}{\zeta_0}\right) \frac{g(\zeta,a)\cos\zeta z}{(k^2-\zeta^2)\bar{K}_{\mathrm{ex}}(\zeta,a)}. \tag{B1}$$

Because of (B1), (6), and (15), eqn. (A2) continues to hold. Thus, similarly to (A3), we can write $I^{(\infty)}_{\mathrm{ex,smfr}}(z)/V$ as a Cauchy Principal Value integral, whose integrand is purely imaginary when $\zeta > k$. It follows that

$$\mathrm{Re}\left\{\frac{I^{(\infty)}_{\mathrm{ex,smfr}}(z)}{V}\right\} = \int_0^k \mathrm{Re}\{r(\zeta)\}\,d\zeta. \tag{B2}$$

With (B1), (2), (14), and the Wronskian relation

$$J_1(t)Y_0(t) - J_0(t)Y_1(t) = \frac{2}{\pi t} \tag{B3}$$

[23, 9.1.16], one can calculate $\mathrm{Re}\{r(\zeta)\}$ and (18) readily follows. Here, because of (4) and (16), there was no need to initially assume $z \neq 0$—one has exponential convergence for all real z.

APPENDIX C. DERIVATION OF (20)

There are only minor differences between the derivation of (20) and that of (18) (Appendix B). Assume, initially, that $z \neq 0$. From (13), the integrand of $I^{(\infty)}_{\mathrm{ap,smfr}}(z)/V$ is

$$r(\zeta) = \left(-\frac{2ika}{\zeta_0}\right) \frac{g(\zeta,a)\cos\zeta z}{(k^2-\zeta^2)\bar{K}_{\mathrm{ap}}(\zeta,a)}. \tag{C1}$$

It is readily checked that the arguments of Appendix B continue to hold: A principal-value integral representation for $I^{(\infty)}_{\mathrm{ap,smfr}}(z)/V$ is possible once again, and the real part of this quantity is $\int_0^k \mathrm{Re}\{r(\zeta)\}\,d\zeta$.

One can find $\mathrm{Re}\{r(\zeta)\}$ from (C1), (1), (14), and the Wronskian relation (B3); $\mathrm{Re}\{r(\zeta)\}$ here turns out to be identical to the corresponding quantity of Appendix A (but differs from that in Appendix B). The initial assumption $z \neq 0$—necessary because of the conditional convergence in (13)—can be removed in the real part discussed herein, but not in the imaginary part.

REFERENCES

1. Fikioris, G. and T. T. Wu, "On the application of numerical methods to Hallén's equation," *IEEE Trans. Antennas Propagat.,* Vol. 49, 383–392, Mar. 2001.
2. Fikioris, G., J. Lionas, and C. G. Lioutas, "The use of the frill generator in thin-wire integral equations," *IEEE Trans. Antennas Propagat.,* Vol. 51, 1847–1854, Aug. 2003.
3. Balanis, C. A., *Antenna Theory: Analysis and Design,* 2nd ed., John Wiley & Sons, New York, 1997.
4. Stutzman, W. L. and G. A. Thiele, *Antenna Theory and Design,* 2nd ed., John Wiley & Sons, New York, 1998.
5. Wu, T. T., "Introduction to linear antennas," *Antenna Theory, Part I,* R. E. Collin and F. J. Zucker (Eds.), Ch. 8, McGraw-Hill, New York, 1969.
6. Fikioris, G., "The approximate integral equation for a cylindrical scatterer has no solution," *J. of Electromagn. Waves and Appl.,* Vol. 15, No. 9, 1153–1159, 2001.
7. Schelkunoff, S. A., *Advanced Antenna Theory,* Section 5.5, John Wiley & Sons, New York, 1952.
8. Fikioris, G., "An application of convergence acceleration methods," *IEEE Trans. Antennas Propagat.,* Vol. 47, No. 12, 1758–1760, Dec. 1999.
9. Stratton, J. A. and L. J. Chu, "Steady state solutions of electromagnetic field problems, I, Forced oscillations of a cylindrical conductor," *J. Appl. Phys.,* Vol. 12, 230–235, 1941.
10. Chen, Y. M. and J. B. Keller, "Current on and input impedance of a cylindrical antenna," *Journal of Research of the National Bureau of Standards—D. Radio Propagation,* Vol. 66D, No. 1, 15–21, Jan.–Feb. 1962.
11. Wu, T. T., "Input admittance of infinitely long dipole antennas driven from coaxial lines," *J. Mathematical Phys.,* Vol. 3, No. 6, 1298–1301, Nov.–Dec. 1962.
12. Fante, R. L., "On the admittance of the infinite cylindrical

antenna," *Radio Sci.,* Vol. 1 (new series), No. 9, 1041–1044, Sept. 1966. Erratum, *Radio Sci.,* Vol. 1 (new series), No. 10, 1234, Oct. 1966.

13. Otto, D. V., "The admittance of cylindrical antennas driven from a coaxial line," *Radio Sci.,* Vol. 2 (new series), No. 9, 1031–1042, Sept. 1967.
14. Miller, E. K., "Admittance dependence of the infinite cylindrical antenna upon exciting gap thickness," *Radio Sci.,* Vol. 2 (new series), No. 12, 1431–1435, Dec. 1967.
15. Andersen, J. B., "Admittance of infinite and finite cylindrical metallic antenna," *Radio Sci.,* Vol. 3 (new series), No. 6, 607–621, June 1968.
16. Otto, D. V., "The admittance of infinite cylindrical antennas," *IEEE Trans. Antennas Propagat.,* Vol. 17, 234–235, March 1969.
17. Richmond, J. H., "Admittance of infinitely long cylindrical wire with finite conductivity and magnetic-frill excitation," *IEEE Trans. Antennas Propagat.,* Vol. 27, 264–266, March 1979.
18. King, R. W. P. and G. S. Smith, *Antennas in Matter,* Section 8.5, MIT Press, Cambridge, MA, 1986.
19. Do-Nhat, T. and R. H. MacPhie, "Effect of gap length on the input admittance of center fed coaxial waveguides and infinite dipoles," *IEEE Trans. Antennas Propagat.,* Vol. 35, 1293–1299, Nov. 1987.
20. Chen, K. C. and L. K. Warne, "Uniform formulas for infinite antenna current," *Radio Sci.,* Vol. 28, No. 5, 649–661, Sept.–Oct. 1993.
21. Morris, M. E. and T. T. Wu, "Admittance of thin, coaxially-friven, infinite monopole antennas," *J. of Electromagn. Waves and Appl.,* Vol. 10, No. 5, 643–692, 1996.
22. Williamson, A. G., "Admittance correction factor for coaxially excited cylindrical antennas," *IEEE Trans. Antennas Propagat.,* Vol. 49, 640–644, April 2001.
23. Abramowitz, I. and I. A. Stegun (Eds.), *Handbook of Mathematical Functions with Formulas, Graphs, and Mathematical Tables,* National Bureau of Standards Applied Mathematics Series, Vol. 55, U.S. Government Printing Office, Washington, D.C., 1972.
24. King, R. W. P., G. Fikioris, and R. B. Mack, *Cylindrical Antennas and Arrays,* Section 13.6, Cambridge University Press, Cambridge, UK, 2002.
25. Werner, D. H., "A method of moments approach for the efficient and accurate modeling of moderately thick cylindrical wire antennas," *IEEE Trans. Antennas Propagat.,* Vol. 46, 373–382,

Mar. 1998.

26. Ablowitz, M. J. and A. S. Fokas, *Complex Variables. Introduction and Applications,* 2nd Ed., Section 4.3, Cambridge University Press, Cambridge, UK, 2003.
27. Gakhov, F. D., *Boundary Value Problems,* Chapt. I, Dover Publications, New York, 1990.
28. Mosig, J. R. and A. A. Melcón, "Green's functions in lossy layered media: Integration along the imaginary axis and asymptotic behavior," *IEEE Trans. Antennas Propagat.,* Vol. 51, 3200–3208, Dec. 2003.

George Fikioris received the Diploma of Electrical Engineering from the National Technical University of Athens, Greece (NTUA) in 1986, and the S.M. and Ph.D. degrees in Engineering Sciences from Harvard University in 1987 and 1993, respectively. From 1993 to 1998, he was an electronics engineer with the Air Force Research Laboratory, Hanscom AFB, MA. He is currently a Lecturer at the School of Electrical and Computer Engineering, NTUA. He is the author or coauthor of over 20 papers in technical journals. Together with R. W. P. King and R. B. Mack, he has authored Cylindrical Antennas and Arrays, Cambridge University Press, 2002. His research interests include electromagnetics, antennas, and applied mathematics. Dr. Fikioris is a Senior Member of the IEEE and a Member of the American Mathematical Society, and of the Technical Chamber of Greece.

Constantine A. Valagiannopoulos was born in Athens, Greece, on March 6, 1982. He graduated from the School of Electrical and Computer Engineering of the National Technical University of Athens in July 2004. He is now with Microwave and Fiber Optics Laboratory and working toward the Ph.D. Degree at the same School. His research interests include electromagnetics, microwaves, propagation, and applied mathematics.